Viscoelastic Characterization of Porcine Functional Spinal Units

Corina M. Espelien, Robert S. Salzar

Abstract Lower back pain (LBP) is a wide-spread, complex and poorly understood issue. In the spine, the disc may be a contributor to LBP based on how it can dictate the displacement response of the spine. This study investigated the creep response to a prescribed stress history of vertebra-disc-vertebra sections of porcine spine. Specimens were exposed to a low-magnitude static compressive hold or a sinusoidal cyclic compression at 4 Hz. In static loading, functional spinal units (FSUs) without the posterior column experience higher strain than those with the posterior column (by approximately a third); in cyclic loading, the overall strain response, with or without the posterior column, is similar. A simple analytical model was fit to the static data and predicted the response of the static loading with the posterior column reasonably well, but it under-predicted the strain for specimens without the posterior column.

Keywords Compression, Fatigue, Porcine, Spine, Viscoelasticity.

I. INTRODUCTION

Lower back pain (LBP) is an issue that affects many individuals, with an estimated 80% of the population experiencing LBP at some point in their lives [1]. Additionally, LBP creates a high cost to society, with a conservative estimate of directly related costs totaling around $20 billion annually [2] and accounting for 20–30% of worker compensation claims in industrialized countries [3]. LBP is a complex issue with causes that are difficult to identify; however, there is compelling evidence linking intervertebral disc (IVD) degeneration to LBP through several observational volunteer studies [4-6]. IVD degeneration can cause IVD height loss and stiffening; therefore, studying the structural response from varying biomechanical exposures could help identify which factors change the extent of IVD height loss or stiffening.

Within the military theatre, helicopter aircrew are exposed to vibrational loadings transmitted through the seat in the rotorcraft; additionally, aircrew are known to have LBP with spine degeneration [7]. While there are multiple factors that could contribute to disc degeneration, this study focused on the contribution of vibration to disc strain. Testing was also performed statically to create a reference strain level for compression of the same duration, but without cyclic loading. Some specimens were prepared by removing the posterior column of the vertebra, which eliminated the pathway for force transmission through the facet joints. A comparison of specimens with and without the posterior column provided insight into the relative proportion of load transmitted through the facet joints.

The experimental specimens selected for this study were porcine functional spinal units (FSUs), otherwise known as motion segments, which consist of vertebrae-disc-vertebrae sections. The discussion section of this study will comment on the justifications and limitations of this species choice. FSUs have been used to examine the response of IVDs since the 1950s. Uniaxial compression is the most frequently explored loading mode, with more than 40 studies characterizing the effective response of post-mortem human subject (PMHS) FSUs [8]. Roughly a quarter of these studies included dynamic or vibrational loading and focused on defining resonant frequencies, phase angles, or dynamic stiffnesses of the IVD in a healthy or degenerative state. This study aimed to elucidate the differences between the cyclic and static loading cases for specimens with and without posterior elements by examining strain-time histories and comparing the predictions of an analytical viscoelastic model to the averaged experimental curves.

C. M. Espelien (e-mail: cme2kd@virginia.edu; tel: +1-434-297-8050) is a PhD student in Mechanical Engineering and R. S. Salzar is an Associate Research Professor of Mechanical and Aerospace Engineering at University of Virginia, USA.

II. METHODS

Specimen Preparation

To test the material response of the IVD with physiological boundary conditions, FSUs were selected as the experimental specimen. Four full porcine spines (Animal Technologies, Tyler, TX, USA), within a mass range of 68 – 91 kg, were purchased for FSU testing. All spines were frozen within 24 hours of harvesting and remained frozen until specimen preparation was initiated. Several studies have shown that a single freeze-thaw cycle does not have a large effect on the overall behaviour of the IVD [8]. All soft tissue was removed from the spines while preserving ligamentous structures. The spine was sectioned into FSUs by cutting at the alternating IVDs (Fig. 1). It should be noted that porcine spines commonly have six lumbar vertebrae; all four porcine spines included in this study had six vertebrae, for a total of twelve FSUs.

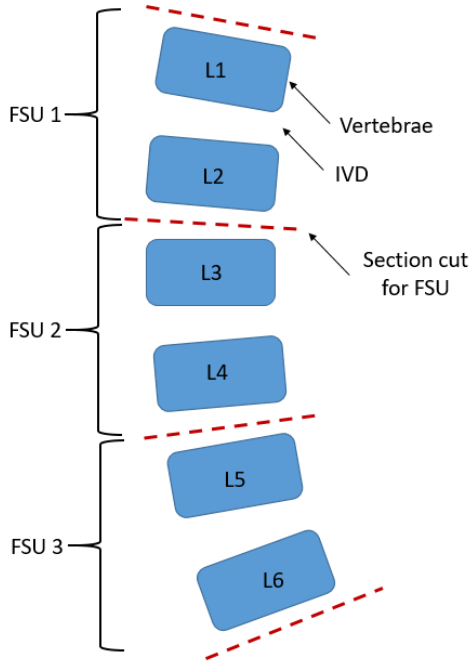

Fig. 1. A schematic of the porcine lumbar spine with the section cuts to obtain FSUs.

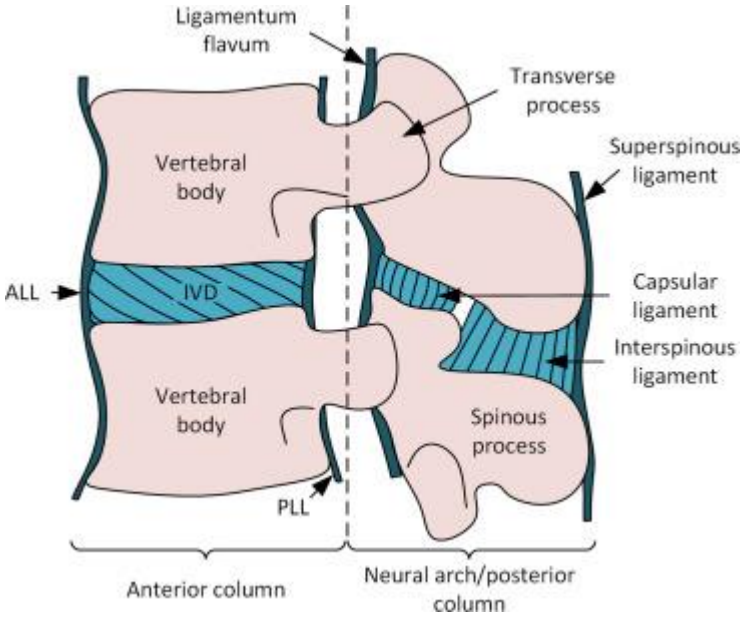

Fig. 2. An illustration of an FSU, illustrating the posterior column [8].

For half of the FSUs, the posterior column, including the processes and facets, were removed (Fig. 2). Removing the posterior column on some of the test specimens was an investigation into how much of an axial load was shunted through bony interactions of the facet joints compared to the load transferred directly through the disc. Portions of each of the superior and inferior vertebrae of each FSU were potted in Fast Cast #891 (Golden West Manufacturing, Inc., Grass Valley, CA, USA), ensuring the endplates and disc being evaluated were free. During potting, care was taken to align the centreline of the IVD with the planes of the inferior and superior potting cups. Pre- and post-test computed tomography images (CTs) were performed on each potted FSU. After potting and up to testing, the specimens were wrapped in saline-soaked gauze and stored in a refrigerated unit.

Specimen Loading and Data Collection

FSU specimens were removed from a refrigerated unit and heated in a water bath in a double bag (specimens were not in contact with or hyper-hydrated by the water). Specimens were vertically loaded on an Instron servo-hydraulic fatigue testing system (Model 8874, Instron Co., Norwood, MA, USA) (Fig. 3). The test system was capable of both force- and displacement-control in uniaxial compression and tension. A custom assembly was designed and built for the potting attachment to the Instron.

During loading of the specimen onto the Instron, the superior pot was attached first to the actuator head, with the inferior pot suspended (not attached to any other equipment, but with weight supported by research personnel). The actuator head and potted specimen were slowly lowered and the inferior potting cup was allowed

to move in the plane normal to the actuator as it come into contact with the base of the Instron. This method allowed for the specimen to self-align relative to the actuator head and minimize any induced flexion, extension, lateral bending, or torsion; it was subsequently attached to the base of the Intron with sliding machining clamps. During loading, the specimen was subjected to minor compression to ensure that all plates and fixtures were flush with the actuator and table. This initial compressive load was typically less than 100 N. After the specimens were appropriately attached in the rig, the FSU was sprayed with saline. The specimens were enclosed in a custom-built environmental chamber to maintain temperature (25.83 +/-3.57°C) and moisture for the duration of the test.

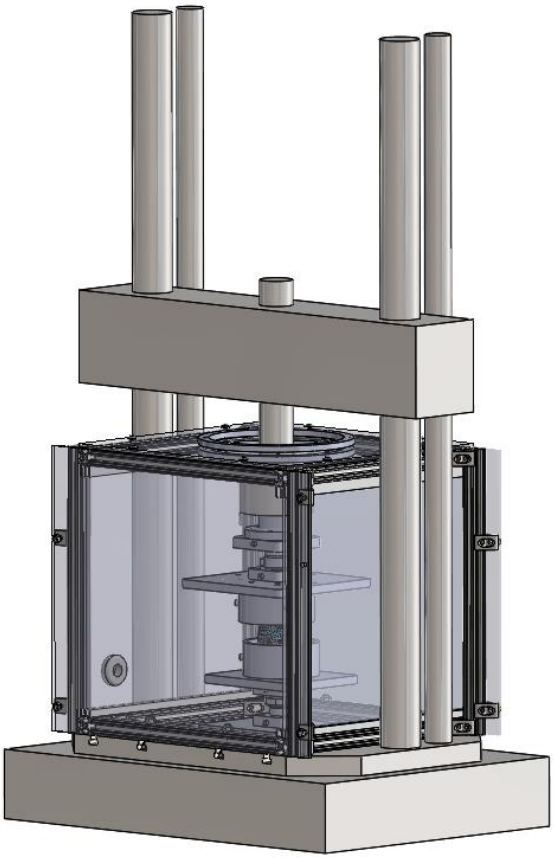

Fig. 3. The custom-built fixtures and environmental chamber integrated with the Instron.

Test Matrix and Input Curves

All testing was performed in force-control of the Instron. Force-control, rather than displacement-control, was chosen because IVDs are exposed to sustained loads, but rarely constant displacements, *in situ*. Table I shows the loading steps, with a description of corresponding magnitudes and durations. The magnitudes are compressive and reported as negative.

The ramp compressed the FSU from the initial force due to setup and specimen loading to -286 N. Preconditioning was performed at the same magnitude as the main loading, but at a lower frequency. Similar to previous studies, preconditioning was used to mitigate any hyper-hydration, freezing and immobility effects accrued after harvesting and during storage [8]. Additional commentary on precondition is provided in the discussion section. The actuator then ramped to 0 N load and stepped to -286 N. The stress step was programmed to be as steep as possible, but due to limitations innate in any equipment, a perfect step is not practically possible. The stress step from 0 N to -286 N occurred in less than 0.1 seconds for all cases. Each specimen was assigned an input of either static loading or dynamic loading. The loading assignments were not based on FSU level. After the three hours of the static or dynamic input, the actuator unloaded via a ramp to 0 N over 10 minutes.

The main compression was varied to be either static or cyclic. The magnitude of the dynamic compression was determined by a mathematical dynamic model, MADYMO (TASS International, Helmond, Netherlands) simulation

for a seated passive male 50th percentile HBM. An experimentally measured load of a rotorcraft seat of 0.4 g axial seat load at 4 Hz was applied to the seatpan of the MADYMO model [9] (Fig. 4). The seatpan was constrained to only move in the axial direction. The seated HBM was constrained by a head strap, shoulder belts, lap belts and knee belts, which were coupled to the seat, to maintain the posture of the passive model. The kinematics of the HBM were not subject to any other constraints. The resulting T12-L1 force curve was obtained and used as a representative load on the lumbar spine. It should be noted that the load magnitude was derived from a human computational model but applied to a porcine experimental specimen. While the porcine specimens were roughly matched to a 50th percentile male mass, there are anatomic differences between porcine and human IVDs, most obviously the disc height and cross-sectional area. This study analyzed stress and strain, which are geometrically-normalized analogs to the raw input force and resultant displacement. Further commentary on the use of a porcine model is included in the discussion section. The results of this study should be considered in terms of the trends of strain between specimens exposed to a static load and those exposed to a dynamic load. Like all biomechanical studies that use human surrogates, context and caution should be used when interpreting the actual numerical values derived from animal models. The static load was defined as the neutral axis of the dynamic load and roughly equivalent to the effective mass of the upper torso (286 N, or approximately 29 kg).

TABLE I
LOAD CURVE STEPS

Waveform Sequence	Magnitude	Duration
Ramp Load	To -238 N	10 seconds
Precondition	-286 N +/- 200 N (1 Hz)	10 minutes (600 cycles)
Ramp Unload	-286 N to 0 N	10 seconds
Stress Step	0 to -286 N	----
Varied Input*	*Static*	
	-286 N	180 minutes
	Dynamic	
	-286 N +/-144 N (4 Hz)	180 minutes (43200 cycles)
Ramp Unload	-286 N to 0 N	10 minutes

*For the varied input step, either the static or dynamic condition was applied.

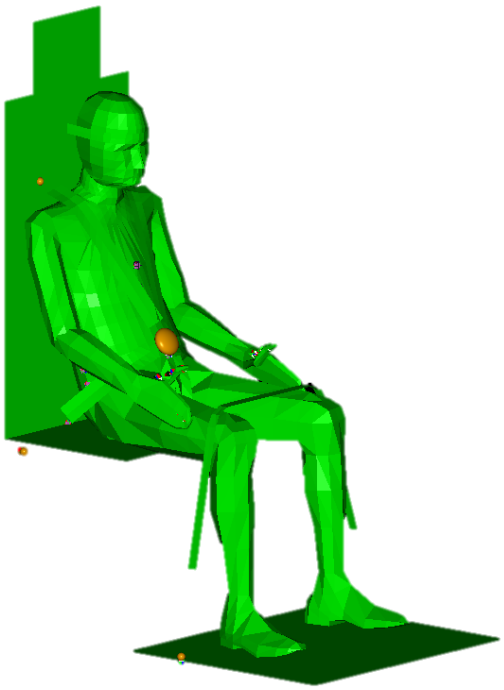

Fig. 4. The seated passive male 50th percentile male model in MADYMO. Vibrational seat-pan acceleration was applied to determine the effective load on the lumbar spine, accounting for recruitment of the upper body.

Data Post-Processing

The pre-testing CTs were analyzed to determine and quantify any off-axis tilt between the IVD and the potting. The off-axis angle tilt, which was an average of 3.61°, was used in a simple transformation to correct the data to examine axial effects only. The load and position data used for stress and strain time histories were only from the static or dynamic input (the ramp, preload and unload data were not analyzed). The potting assembly and material, as well as the vertebral bodies, were treated as rigid bodies for this analysis. This assumption means that all displacements were contributable to the IVD. All strains and stress reported are engineering strains and stresses, using the initial disc height and cross-sectional area from the pre-test CTs. The average (+/- standard deviation) IVD disc height was 4.62 mm (+/- 0.72 mm) and cross-sectional area was 698.54 mm^2 (+/- 48.08 mm^2) for the specimens. For each of the cyclic experimental curves, the minimum and maximum point from each cycle were averaged to create a smooth trendline of the cyclic data. The resulting trendline was used as a representation of the overall creep of the cyclic tests.

Material Model Fitting

In this analysis, the effective behaviour of the entire IVD was considered; the individual components of the annulus fibrosis layers and nucleus pulposus were not modelled or summed into a cumulative response. Time-dependent behaviour was easily observable in the IVD displacement response, therefore a constitutive model that predicted creep behaviour was necessary. The analytical model chosen for material fitting was a general Kelvin model, which consists of n number of spring-damper sets (in parallel orientation) aligned in series (E1, η1), with one additional spring in series (E2). For this analysis, n=1, meaning only one time constant was considered. This simplified model is also known as a Kelvin representation of the standard linear model. Previous studies have used this model when there is a known applied initial stress and time-dependent behaviour [10,11]. The model has three material parameters that can be optimized. Additionally, the model includes the initial stress-step as part of its formulation.

III. RESULTS

Strain Response with and without Posterior Column for Static Loading

Table II shows the average strains after one hour, two hours, and three hours (end of test) for specimens with the posterior column and for specimens without the posterior column for static and cyclic loading.

TABLE II
AVERAGE STRAINS (%)

Specimens Included in Average	60 Minutes	120 Minutes	180 Minutes
With Posterior Column - Static	14.69	19.77	22.22
Without Posterior Column - Static	22.01	30.12	33.36
With Posterior Column - Cyclic	16.35	22.47	25.80
Without Posterior Column - Cyclic	16.88	22.50	25.79

Curve Fitting

From the static averaged curves and using the generalized Kelvin model, a least-squares optimization was performed to determine the coefficients, E1, η1, and E2, set out in Table III. The experimental average and predicted model curves for static loading are shown in Fig. 5. The model was compared to the averaged experimental cyclic responses in Fig. 6.

TABLE III
MODEL PARAMETERS

Specimens Included in Average	E1 (MPa)	η1 (MPa s)	E2 (MPa)
With Posterior Column	1.75	5742.71	49.57
Without Posterior Column	1.22	4404.79	53.05

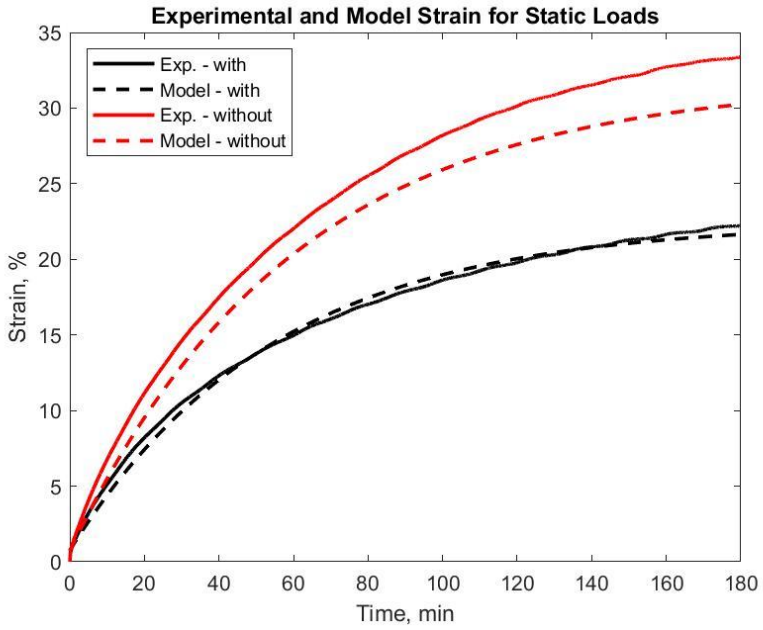

Fig. 5. The strain for the average static experimental and fitted model for the specimens with and without the posterior column.

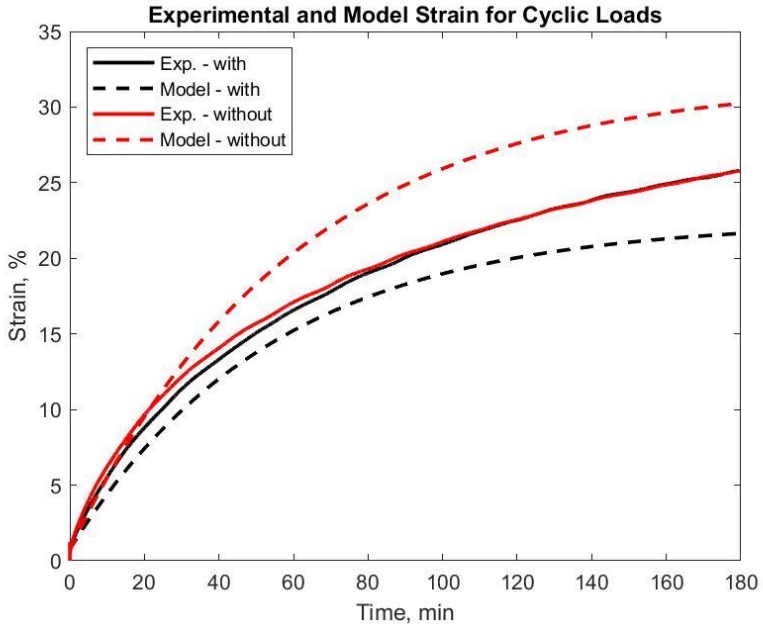

nFig. 6. The strain for the average cyclic experimental and fitted model for the specimens with and without the posterior column.

IV. Discussion

The specimens with the posterior column resulted in roughly 33% less strain than the specimens without the posterior column based on the average static experimental curves for 60 minutes, 120 minutes and 180 minutes. This indicates that the facet interactions cannot be neglected when considering the displacement response in static uniaxial compression of the spine, even with the vertebra-IVD-vertebra segments considered here. The average strains for the cyclic loading curves were approximately the same for the average with and without the posterior column. There could be multiple reasons for a difference between specimens with and without the posterior column in the static tests but no difference in the cyclic tests. In the static tests, the effect of a small instability could have been perpetuated under the constant compressive force and resulted in a larger end strain for the specimens without the posterior column. For the static tests of specimens with a posterior column, the

facet joints may have provided stabilization in addition to a supplemental load path. In the cyclically loaded specimens, the less compressive portion of the loading (smaller magnitude than 286 N) could have allowed for some small realignment of the internal structure of the disc, like the fibers of the annulus fibrosis, that increased the stability, that there was not a large difference between the specimens with and without the posterior column. Such instabilities could have been due to non-axial forces, like shearing. It should be noted that no gross damage of the disc was observed visually or via CT for any specimens after testing, nor were there any large perturbations in the data traces. Any instabilities did not result in catastrophic failure of the disc.

The analytical generalized Kelvin model under-predicted the end strain for the static loading cases, although it did compare well to the data for the specimens with the posterior column. The model from the static testing did not predict the experimental strain from cyclic load cases well for either the average with the posterior column or the average without the posterior column. The experimental average curves for the cyclic cases were similar, with almost identical strains at the end of test (3 hours).

The difference between the average static curves with the posterior column and without the posterior column could be due to one outlier curve, for specimen 3, FSU 01 (an FSU without the posterior column) that reached very high strain (36.55% strain). A larger sample size for all categories would provide additional insight into whether the trends displayed here remain consistent.

There are several limitations to the presented work. The specimens selected were porcine FSUs, prepared with and without the posterior column. FSUs themselves are not representative of the dynamic kinematics or kinetics of a full *in vivo* spine; however, they do allow for a more isolated examination of an individual IVD. Specimens were tested with and without the posterior column in a further attempt to isolate the response of the disc, as loads in compression can be partially shunted through the facet joints. The removal of the posterior column may have disrupted the integrity of the specimen and let to instability that is not representative of an *in vivo* spine. This instability was reflected by a larger spread of data for the specimens without the posterior column.

Porcine, rather than PMHS, specimens were used as a surrogate for this tissue testing. Scaling between species remains a challenge in the biomechanics field for almost all body regions and applications. Canine, ovine (sheep, goat), porcine and bovine spines of varying species and maturity have been routinely used as large animal options for human surrogates [12,13]. Other animals, such as kangaroos, deer, baboons, and other primates, can be used, but they are less common [12,14,15]. Considerations when using an animal surrogate are differences from humans in anatomy, physiological loading, range of motion and material properties. By initial observation, it is difficult to justify a quadruped as a surrogate for a biped in spine mechanics. However, studies with different approaches including the analysis of muscle and ligament forces, trabecular bone density and intradiscal pressure have shown that quadrupeds do experience significant axial loading of the spine [16]. Sheep have been accepted as a surrogate for human spine biomechanics, especially when considering various ranges of motion [16,17]. However, there is evidence that disc mechanics in the axial direction are preserved across several species, including pigs, when assessing geometrically-normalized measures such as stress and strain [18]. Furthermore, the facet anatomy of immature pigs (55-65kg), which are roughly weight-matched to the average human male, more closely resembles human facets compared to dogs, micropigs, sheep and goats [13]. Animal surrogates always have limitations, but an immature, weight-matched porcine model is acceptable for the axial loading case examined in this study, regardless of if the posterior column, which includes the facet joints, is removed or preserved.

It was assumed that all loading and subsequent analysis was only in the axial direction. Despite the mitigations taken during potting and loading the specimen, as well as the correctional factors used during data analysis, there could be forces and moments that were applied to the specimen and not captured during data acquisition. These forces and moments could have been contributors to the spread of data. Recommendations for similar studies are the use of a more robust self-aligning testing equipment and data collection on multi-directional forces and moments to supplement the on-board instrumentation of uniaxial testing systems like an Instron. Inertial compensation was not considered in this analysis. The load cell used to acquire data was coupled with the actuator of the Instron and could have been subject to error due to inertial artifacts. Since this experimental work was performed in force-control, an exact replicate unloaded test would not be possible since the compressive targets for each waveform step would never be achieved. However, an approximate displacement-control waveform sequence based on previously acquired data could have been generated to estimate the inertial effects and needed compensation of a moving force sensor. Hysteresis was not examined in this study for the cyclic

specimens. The aim of this study was to compare the strain of a long-term compressive stress in a static and cyclic testing mode. The data from each individual cycle in the cyclic testing cases did not have an analog in the static testing cases; instead, the static creep and effective cyclic creep, which required a smoothed trendline of the cyclic data, were compared. The chosen loading scheme had limitations. The prescribed motion was force-controlled, rather than displacement controlled. While material analysis can be performed based on input force or stress, analytical models are primarily presented with an input displacement and resultant forces. The constitutive model can be inverted to allow for an input displacement and resultant force but may present difficulties when comparing to other experimental and analytical work in literature. Additionally, the input was always the same force, rather than the same stress. While prescribing a stress or strain, rather than a set force or displacement, can be cumbersome to do experimentally, it is possible the prerequisite knowledge based on pre-testing imaging to obtain specimen-specific geometric data. The chosen waveforms themselves were not a data trace taken directly from the field; instead, experimental acceleration of a rotorcraft seatpan was applied to a multibody model which was validated to capture global spine behaviour, from which an interspinal load was obtained. This study used the intermediate step of a computational model to gain insight into what the interspinal loads from whole body loading could be, but the biofidelity of interspinal loads in the model are not validated. *In vivo* interspinal loads are difficult to obtain experimentally due to testing logistics, ethics and species-scaling considerations.

The decision to precondition and the extent of preconditioning remains a point of contention within the field of soft tissue testing. Preconditioning is intended to reduce variability of testing, since hysteresis is greatest during the first complete loading cycle. Different approaches recommend a set number of preconditioning cycles, ranging from three to thousands, while others recommend real-time assessment of one cycle at a time [8,19]. Additionally, the rest between the preconditioning and the testing of interest can also be considered [20]. The magnitude of the preconditioning can also be varied. In the field of injury biomechanics, it is obvious that preconditioning magnitudes should never exceed the testing magnitude; however there is less innate clarity when low magnitude loads that are closer to a daily physiological exposure are being tested. Some recommend preconditioning soft tissues to the maximum strain being tested, while others recommend physiologic preconditioning for IVDs, specifically, to avoid the effects of hyper-hydration during unloaded storage [21,22]. Furthermore, this study aimed to investigate differences in strain between static and cyclic loading conditions. The preconditioning for both testing groups was equivalent; the trends between the two testing groups was likely unaffected by the level of preconditioning. The level of preconditioning could have affected the overall shape and magnitude of all the resulting strain curves, but roughly to the same extent.

Lastly, this study only focused on how vibrational loading could affect the strain compared to a static loading case in the lumbar spine with the clinical motivation of examining IVD degeneration in rotorcraft aircrew. The seatpan vibration the aircrew experience could be one of many factors that increases their incidence and severity of IVD degeneration and LBP. For rotorcraft aircrew, especially pilots, additional biomechanical considerations are the awkward postures that must be maintained, additional mass due to headgear and other equipment, rest time between flights, time of day of flights (IVD height changes throughout the day), as well as previously accumulated flight exposures and overall IVD degeneration.

V. CONCLUSIONS

A simple analytical model can predict the time-dependent creep behaviour of FSUs with the posterior column in uniaxial static compression reasonably well. In static loading, FSUs without the posterior column experience higher strain than those with the posterior column; in cyclic loading, the overall strain response, with or without the posterior column, is similar. Future work should include a comparison between porcine and PMHS experimental data and analytical model predictions to assess the cross-species scalability.

VI. Acknowledgement

This effort was funded by MTEC Research Project No. MTEC-18-04-I-PREDICT-07, sponsored by the Office of Naval Research. The views and conclusions contained herein are those of the authors and should not be interpreted as necessarily representing the official policies or endorsements, either expressed or implied, of the U.S. Government.

VII. References

[1] Zhang, Y., Guo, T. M., Guo, X., Wu, S.X. (2009). Clinical diagnosis for discogenic low back pain. *International Journal of Biological Sciences*, 2009, **5**(7): pp.647–658.

[2] Katz, J. N. (2006) Lumbar disc disorders and low-back pain: socioeconomic factors and consequences. *Journal of Bone and Joint Surgery*, 2006, **88**(2): pp.21–24.

[3] Kerr, M. S., Frank, J. W., *et al.* (2001) Biomechanical and psychosocial risk factors for low back pain at work. *American Journal of Public Health*, 2001, **91**(7): pp.1069–1075.

[4] Luoma, K., Riihimäki, H., *et al*. (2000) Low back pain in relation to lumbar disc degeneration. *Spine*, 2000, **25**(4): pp.487–492.

[5] Salminen, J. J., Erkintalo, M. O., Pentti, J., Oksanen, A., Kormano, M. J. (1999) Recurrent low back pain and early disc degeneration in the young. *Spine*, 1999, **24**(13): p.1316.

[6] Battié, M. C., Videman, T., Levalahti, E., Gill, K., Kaprio, J. (2007) Heritability of low back pain and the role of disc degeneration. *Pain*, 2007, **131**(3), pp.272–280.

[7] Byeon, J. H., Kim, J. W., *et al.* (2013). Degenerative changes of spine in helicopter pilots. *Annals of rehabilitation medicine*, 2013, **37**(5), 706.

[8] Newell, N., Little, J. P., *et al*. (2017) Biomechanics of the human intervertebral disc: a review of testing techniques and results. *Journal of the Mechanical Behaviour of Biomedical Materials,* 2017, **69**: pp.420–434.

[9] Hiemenz, G. J., Hu, W., Wereley, N. M. (2008) Semi-active magnetorheological helicopter crew seat suspension for vibration isolation. *Journal of Aircraft*, 2008, **45**(3): pp.945–953.

[10] Burns, M. L., Kaleps, I., & Kazarian, L. E. (1984). Analysis of compressive creep behaviour of the vertebral unit subjected to a uniform axial loading using exact parametric solution equations of Kelvin-solid models—Part I. Human intervertebral joints. *Journal of biomechanics*, 1984, **17**(2), 113-130.

[11] Kaleps, I., Kazarian, L. E., & Burns, M. L. (1984). Analysis of compressive creep behaviour of the vertebral unit subjected to a uniform axial loading using exact parametric solution equations of Kelvin-solid models—Part II. Rhesus monkey intervertebral joints. *Journal of biomechanics*, 1984, **17**(2), 131-136.

[12] Brandolini, N., Cristofolini, L., & Viceconti, M. (2014). Experimental methods for the biomechanical investigation of the human spine: a review. *Journal of Mechanics in Medicine and Biology*, 2014, **14**(01), 1430002.

[13] McLain, R. F., Yerby, S. A., & Moseley, T. A. (2002). Comparative morphometry of L4 vertebrae: comparison of large animal models for the human lumbar spine. *Spine*, 2002, **27**(8), E200-E206.

[14] Panjabi, M. M. (1998). Cervical spine models for biomechanical research. *Spine*, 1998, **23**(24), 2684-2699.

[15] Balasubramanian, S., Peters, J. R., Robinson, L. F., Singh, A., & Kent, R. W. (2016). Thoracic spine morphology of a pseudo-biped animal model (kangaroo) and comparisons with human and quadruped animals. *European Spine Journal*, 2016, **25**(12), 4140-4154.

[16] Casaroli, G., Wade, K., Villa, T., & Wilke, H. J. (2018). Animal Models for Spine Biomechanics. *Biomechanics of the Spine* (pp. 279-296). Academic Press.

[17] Wilke, H. J., Kettler, A., Wenger, K. H., & Claes, L. E. (1997). Anatomy of the sheep spine and its comparison to the human spine. *The Anatomical Record: An Official Publication of the American Association of Anatomists*, 1997, **247**(4), 542-555.

[18] Beckstein, J. C., Sen, S., Schaer, T. P., Vresilovic, E. J., & Elliott, D. M. (2008). Comparison of animal discs used in disc research to human lumbar disc: axial compression mechanics and glycosaminoglycan content. *Spine*, 2008, **33**(6), E166-E173.

[19] Costi, J. J., Ledet, E. H., & O'Connell, G. D. (2021). Spine biomechanical testing methodologies: The controversy of consensus vs scientific evidence. *JOR spine*, 2021, **4**(1), e1138.

[20] Carew, E. O., Barber, J. E., & Vesely, I. (2000). Role of preconditioning and recovery time in repeated testing of aortic valve tissues: validation through quasilinear viscoelastic theory. *Annals of biomedical engineering*, 2000, **28**(9), 1093-1100.

[21]Cheng, S., Clarke, E. C., & Bilston, L. E. (2009). The effects of preconditioning strain on measured tissue properties. *Journal of biomechanics*, 2009, **42**(9), 1360-1362.

[22]Dhillon, N., Bass, E. C., & Lotz, J. C. (2001). Effect of frozen storage on the creep behaviour of human intervertebral discs. *Spine*, 2001, **26**(8), 883-888.